

## Oxygen/Glucose Deprivation and Reperfusion Cause Modifications of Postsynaptic Morphology and Activity in the CA3 Area of Organotypic Hippocampal Slice Cultures

Yeon Joo Jung, Eun Cheng Suh, and Kyung Eun Lee

Department of Pharmacology and Ewha Medical Research Institute, Ewha Womans University School of Medicine, Seoul 158-710, Korea

Brain ischemia leads to overstimulation of *N*-methyl-D-aspartate (NMDA) receptors, referred as excitotoxicity, which mediates neuronal cell death. However, less attention has been paid to changes in synaptic activity and morphology that could have an important impact on cell function and survival following ischemic insult. In this study, we investigated the effects of reperfusion after oxygen/glucose deprivation (OGD) not only upon neuronal cell death, but also on ultrastructural and biochemical characteristics of postsynaptic density (PSD) protein, in the stratum lucidum of the CA3 area in organotypic hippocampal slice cultures. After OGD/reperfusion, neurons were found to be damaged; the organelles such as mitochondria, endoplasmic reticulum, dendrites, and synaptic terminals were swollen; and the PSD became thicker and irregular. Ethanolic phosphotungstic acid staining showed that the density of PSD was significantly decreased, and the thickness and length of the PSD were significantly increased in the OGD/reperfusion group compared to the control. The levels of PSD proteins, including PSD-95, NMDA receptor 1, NMDA receptor 2B, and calcium/calmodulin-dependent protein kinase II, were significantly decreased following OGD/reperfusion. These results suggest that OGD/reperfusion induces significant modifications to PSDs in the CA3 area of organotypic hippocampal slice cultures, both morphologically and biochemically, and this may contribute to neuronal cell death and synaptic dysfunction after OGD/reperfusion.

**Key Words:** Neuronal cell death, NMDAR, OGD/reperfusion, Organotypic hippocampal slice cultures, Postsynaptic density

### INTRODUCTION

During brain ischemia, the lack of energy induces a collapse of ionic gradients, followed by excessive presynaptic neuronal depolarization, abnormal release of excitatory neurotransmitters, and a reduced reuptake of these neurotransmitters from the extracellular space. Glutamate is the major excitatory neurotransmitter in the brain, and an increased level of glutamate induces overstimulation of *N*-methyl-D-aspartate receptors (NMDARs) in the post-synapse, a massive influx of  $\text{Ca}^{2+}$ , pathological synaptic plasticity, and the subsequent activation of cell death signaling pathways. This overstimulation of NMDARs is commonly referred to as excitotoxicity, and is assumed to be

a critical mechanism in the neuronal death that occurs following an ischemic insult [1-4].

Most studies into ischemia have focused primarily on the mechanism of cell death or survival, while much less attention has been paid to the activity and morphology of synapses, which could have an important impact on cell function and survival [5-7].

Postsynaptic density (PSD) is a postsynaptic scaffold harboring several different receptor complexes, which directly participate in synaptic transmission [8-11]. In the mammalian CNS glutamatergic synapse, a typical PSD is composed of a large, complex protein network consisting of several hundred different proteins, in which members of the membrane-associated guanylate kinase (MAGUK) family are of crucial importance [12-15].

The PSD is composed of four major types of molecules: membrane-bound, cytoskeletal, and scaffolding proteins, as well as modulatory enzymes. The most abundant membrane-bound proteins found in the PSD are NMDARs, while the abundant cytoskeletal elements, including actin, are important in localizing and clustering the PSD receptors and signal complexes [16]. Scaffolding proteins, including

Received August 30, 2012, Revised October 8, 2012,  
Accepted October 20, 2012

Corresponding to: Kyung Eun Lee, Department of Pharmacology, Ewha Womans University School of Medicine, 911-1, Mok-5-dong, Yangcheon-gu, Seoul 158-710, Korea. (Tel) 82-2-2650-5744, (Fax) 82-2-2653-8891, (E-mail) kelee@ewha.ac.kr



This is an Open Access article distributed under the terms of the Creative Commons Attribution Non-Commercial License (<http://creativecommons.org/licenses/by-nc/3.0>) which permits unrestricted non-commercial use, distribution, and reproduction in any medium, provided the original work is properly cited.

**ABBREVIATIONS:** OGD, oxygen/glucose deprivation; PSD, postsynaptic density; PSD-95, postsynaptic density protein 95; NR1, NMDA receptor 1; NR2B, NMDA receptor 2B; CaMKII, calcium/calmodulin-dependent protein kinase II.

PSD-95, bring the various PSD components into association. The key enzymes regulating PSD components include calcium/calmodulin protein kinase II (CaMKII), protein kinase C (PKC), and neuronal nitric oxide synthase (nNOS) [17].

A major component of the PSD fraction is PSD-95, which is the best characterized MAGUK protein. As an essential synaptic adaptor protein, PSD-95 interacts with a large variety of molecules, and thus by physically bringing together cytoplasmic signal transduction proteins and surface receptors, may facilitate the coupling of various signaling cascades within the PSD [11,18-20].

The first molecule identified as binding to the PDZ domain of PSD-95 was the NR2A/B subunit of the NMDAR [21-23]. NMDARs in the mammalian brain are thought to be heterotetramers of two obligatory NR1 subunits, in combination with either NR2A and/or NR2B [24-26].

CaMKII is one of the most abundant proteins in neurons, and is highly concentrated in the PSD at glutamatergic synapses [16,27,28]. It plays a key role in synaptic plasticity [29]. Two isoforms,  $\alpha$ - and  $\beta$ -CaMKII, are neuron specific, and CaMKII shows dynamic translocation to the PSD in response to  $Ca^{2+}$  influx through NMDARs [30].

Therefore, this study aimed to investigate the effects of reperfusion following oxygen/glucose deprivation (OGD) not only upon neuronal cell death, but also on the ultrastructural and biochemical characteristics of PSD proteins in the stratum lucidum of the CA3 area in organotypic hippocampal slice cultures.

## METHODS

### *Preparation of organotypic hippocampal slice cultures*

All surgical and experimental procedures were reviewed and approved by the Institutional Animal Care and Use Committee (IACUC) of Ewha Womans University.

Organotypic hippocampal slice cultures were prepared from the hippocampi of 10-day-old Sprague-Dawley rats [31,32]. Hippocampi were dissected and cut at 300- $\mu$ m thickness using a McIlwain tissue chopper (The Mickle Laboratory Engineering Corporation, UK). The slices were carefully placed onto membrane units (0.4  $\mu$ m; Millipore, MA, USA) in 6-well plate, with each well containing 1.2 ml of a culture medium, as previously described [31], and were incubated at 37°C in 95% O<sub>2</sub>/5% CO<sub>2</sub>.

### *Induction of OGD*

Excitotoxicity and NMDARs contribute to cell death induced by OGD/reperfusion. To achieve the appropriate conditions for NMDAR expression [33], slices were grown in culture for 14 days. After incubation for 14 days, slices were washed with fresh media, and then placed in an OGD buffer pre-gassed with 95% N<sub>2</sub>/5% CO<sub>2</sub>, and then incubated at 37°C in 95% N<sub>2</sub>/5% CO<sub>2</sub> for 30 min. After this, the OGD media was replaced with normal, fresh media for up to 24 h during reperfusion. Control slices underwent the same manipulations, but were incubated with fresh normal media instead of OGD media gassed with 95% O<sub>2</sub>/5% CO<sub>2</sub> at 37°C for 30 min.

### *Transmission electron microscopy (TEM)*

Slices were fixed in 2.5% glutaraldehyde at 4°C for 2 h, postfixed in 1% OsO<sub>4</sub> for 1 h, and embedded in an Epon 812. Before ultrathin cutting, the semi-thin sections (2 mm) were cut from the CA3 area of the slices, stained with toluidine blue, and examined under light microscopy. From each semi-thin section, 40~50 ultrathin sections (LKB Ultratome III, Mager Scientific, USA) were cut and stained with 5% uranyl acetate and lead citrate. The preparations were examined using a transmission electron microscope (Hitachi H-600, Hitachi, Tokyo, Japan).

For ethanolic phosphotungstic acid (EPTA) staining [34,35], sections were dehydrated in an ascending series of ethanol up to 100%, and stained for 45 min with 1% phosphotungstic acid (PTA), which was prepared by dissolving 0.1 g PTA in 10 ml of 100% ethanol, and adding 4 drops of 95% ethanol. Sections were then dehydrated in dry acetone, and embedded in Epon 812. Ultrathin sections (0.1  $\mu$ m) were prepared and examined using an electron microscope (Hitachi H-600, Hitachi, Tokyo, Japan).

### *Analysis of postsynaptic densities and morphology*

For analysis of the synapse density and morphology, images were taken from randomly sighted stratum lucidum at a magnification of 5,000 $\times$  for each experimental condition (n=4). The estimation of synapse density was carried out from single photos by counting all synapses (a presynaptic terminal facing a postsynaptic density). For each group, the total pictured area of 1,205~1,507  $\mu$ m<sup>2</sup> was analyzed, and synapse density was expressed as number of synapses per 100  $\mu$ m<sup>2</sup>. For determination of the minimal thickness, maximal thickness, length, and total area of each PSD, the NIH software program Image J was used for morphometric measurements.

### *Western blot analysis*

Western blot analysis was performed according to the method reported Suh et al. [36]. Briefly, slices were homogenized to obtain protein extracts. The protein concentration was measured using the Bradford method, and adjusted with 1% SDS. Equal amounts of protein were subjected to 8~10% SDS-PAGE, electrophoretically transferred onto nitrocellulose membranes, and then blocked with 10% skim milk in TBS containing 0.05% Tween 20 (TBST) for 1 h at room temperature. The membranes were then incubated with either mouse anti-PSD-95 (1 : 1,000; Sternberger Monoclonals, Baltimore, MD), anti-NR1 (1 : 1,000; Sigma Chemical Corporation, St. Louis, MO), mouse anti-NR2B (1 : 500; Millipore, Billerica, MA) or mouse-anti-CaMKII (1 : 1,000; Millipore, Billerica, MA) as a primary antibody for 1 h, and washed three times with TBST (0.05%) for 10 min. Next, the membranes were incubated with a secondary antibody coupled to horseradish peroxidase (HRP) for 45 min. After washing with TBST (0.05%), an enhanced chemiluminescence method (Santa Cruz Biotechnology, Santa Cruz, CA) was used to develop the films. The resulting films were scanned, and densitometric analysis of bands was performed using NIH software program Image J.

**Statistical analysis**

Data are presented as the mean±standard error of the mean (SEM). Statistical differences between groups were determined by one-way analysis of variance (ANOVA) with Fisher's post-hoc test (Statview 5 version, SAS institute, USA). The threshold for statistical significance was set at  $p < 0.05$ .

**RESULTS**

**Neuronal cell death was detected in the CA3 area following OGD/reperfusion**

To determine whether neurons are damaged after

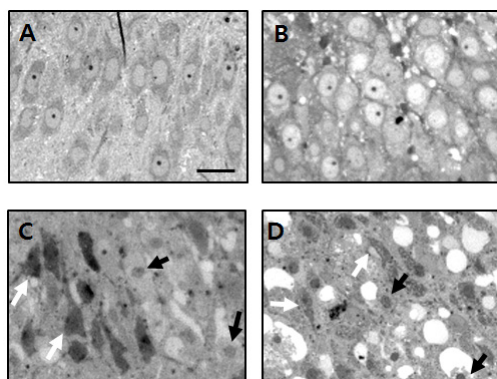


**Fig. 1.** Light micrographs of the CA3 pyramidal cell layer of organotypic hippocampal slice cultures, stained with toluidine blue, after OGD/reperfusion. (A) Control, (B) OGD for 30 min, (C) reperfusion for 6 h after OGD, (D) reperfusion for 24 h after OGD. Neuronal cell death was induced after OGD/reperfusion. Black arrows indicate condensed pyknotic nuclei, and white arrows indicate cells stained dark, with triangular shrunken perikaryon. Scale bar=100  $\mu$ m.

OGD/reperfusion, toluidine blue staining was performed on the organotypic hippocampal slice cultures. In control slices, the neurons of the CA3 pyramidal cell layer had a normal shape, with large cell bodies and clearly visible Nissl bodies (Fig. 1A). After OGD for 30 min, the cell bodies of the CA3 pyramidal cell layer and adjacent tissue appeared swollen (Fig. 1B). At 6 h (Fig. 1C) and 24 h after reperfusion (Fig. 1D), the number of surviving neurons was decreased, and most remaining neurons showed condensed pyknotic nuclei. Some had a triangular, shrunken perikaryon and were stained dark, suggesting that these neurons were damaged.

**OGD/reperfusion induced ultrastructural changes in the stratum lucidum of the CA3 area**

In control slices stained with osmium-uranium-lead, CA3 cells had the typical shape of pyramidal neurons, with large round nuclei, homogeneously dispersed karyoplasm, well developed rough endoplasmic reticulum (ER) and poly-ribosomes, and structurally normal mitochondria (data not shown). Because we targeted the stratum lucidum region of the CA3 area for ultrastructural analysis, there were not many cell bodies present, but many typical dendrites and synapses (presynaptic terminal facing a postsynaptic density). The synapses in control slices were structurally intact with a clear, narrow, synaptic cleft, and many synaptic vesicles located in the presynaptic terminals (Fig. 2A, 2E). After 30 min of OGD, some swelling of the mitochondria, and synaptic terminals was observed. The thickness of the PSD in many synapses became thicker and more electron dense than in controls (Fig. 2B, 2F). At 6 h of reperfusion (Fig. 2C, 2G) and 24 h of reperfusion (Fig. 2D, 2H) the swelling of organelles including mitochondria and neuronal processes, disorganization of the mitochondria and ribosomes, and the thickness and electron density of the PSD were all markedly increased.

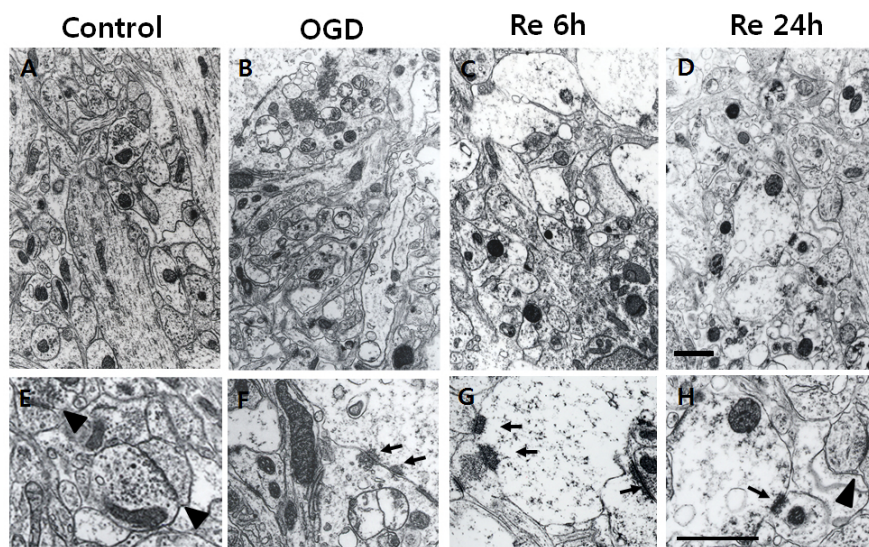


**Fig. 2.** Electron micrographs of osmium-uranium-lead-stained stratum lucidum in the CA3 area of organotypic hippocampal slice cultures after OGD/reperfusion. (A, E) control, (B, F) OGD for 30 min, (C, G) reperfusion for 6 h after OGD, (D, H) reperfusion for 24 h after OGD. (E~H) higher magnification images. In control slices, typical intact synapses with a clear narrow synaptic cleft can be clearly seen (arrowhead). Mitochondria, ER, dendrites, and synaptic terminals were swollen, and the thickness of the PSD in many synapses became thicker (black arrows) in the OGD/reperfusion group than in the controls. Scale bar=2  $\mu$ m.

**The morphology of synapses was remarkably changed in the stratum lucidum of the CA3 area after OGD/reperfusion**

In order to evaluate PSD morphology in the CA3 area after OGD/reperfusion, TEM with EPTA staining was performed. After 30 min of OGD, there were no changes on the number, length, thickness and area of PSDs, and those parameters of PSDs were started to be changed at 6 h after OGD (data not shown). At 24 h after OGD, the number of PSDs was significantly decreased by around 50% ( $13.69 \pm 1.21$  compared to  $27 \pm 3.23$  in controls,  $p < 0.05$ , Fig. 3C). The PSD length at 24 h after OGD was significantly increased by approximately 63% ( $411 \pm 13$  nm compared to  $252 \pm 8$  nm in controls,  $p < 0.05$ , Fig. 3D), and the PSD thickness was also significantly increased by approximately 85% ( $45.1 \pm 1.9$  nm compared to  $24.4 \pm 0.7$  nm in controls,  $p < 0.05$ , Fig. 3E).

In addition, the area of the PSD was prominently increased in compare to control ( $14.19 \pm 1.03 \mu\text{m}^2$  compared to  $4.40 \pm 0.21 \mu\text{m}^2$  in controls,  $p < 0.05$ , Fig. 3F, Table 1).

**Levels of PSD proteins decreased after OGD/reperfusion**

To investigate the effect of OGD/reperfusion on levels of PSD proteins, western blot analysis for PSD-95, NR1,

NR2B, and CaMKII was performed on the hippocampal slice cultures. Levels of all of the analyzed postsynaptic proteins decreased following OGD/reperfusion in a time dependent manner, and showed the lowest levels at 24 h reperfusion after OGD (Fig. 4A & 4B).

**DISCUSSION**

In the present study, our results show that the morphology of the PSD changed, and that levels of major PSD proteins, such as PSD-95, NR2B, NR1, and CaMKII, were all decreased in the CA3 area of organotypic hippocampal slice cultures following OGD/reperfusion.

Brain ischemia triggers complex cellular mechanisms that impair synaptic functions through the breakdown of cellular and structural features, mediated by various excitotoxic signals [35,37,38]. It is well known that the CA1 area of hippocampus is particularly vulnerable to ischemic insult [39,40]. However, various biochemical and pathological activities, followed by neuronal cell death, can also be detected in the CA3 area along mossy fibers [41,42]. According to our previous studies [31,43], neuronal damage expressed with propidium iodide staining was found both in the CA1 area and CA3 area of hippocampal slice cultures following OGD/reperfusion.

Following OGD for 30 min, some swelling of the mi-

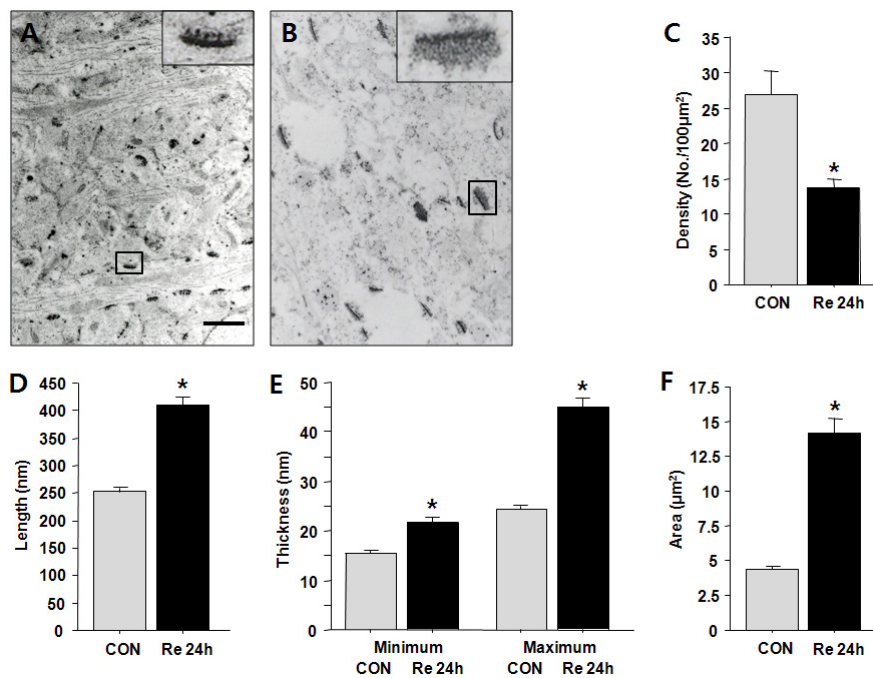


**Fig. 3.** Electron micrographs of EPTA staining of stratum lucidum in the CA3 area of organotypic hippocampal slice cultures after OGD/reperfusion. (A) Control, (B) reperfusion for 24 h after OGD. (C) Synapse density/100  $\mu\text{m}^2$ , (D) length of a PSD, (E) minimum and maximum thickness of a PSD, (F) area of a PSD. In the control slices, many PSDs appeared as thin and compact lines. At 24 h after OGD, the density of PSDs was significantly decreased, and the PSDs became thicker, longer, and more irregular. Insert images are high magnification of the synapses. Scale bar=1  $\mu\text{m}$ . Data are expressed as mean $\pm$ SEM. \* $p < 0.05$  compared to control.

**Table 1.** Quantification of PSDs in CA3 after OGD/reperfusion

Group	Density (No./100 $\mu\text{m}^2$ )	Length (nm)	Minimum thickness (nm)	Maximum thickness (nm)	Area ( $\mu\text{m}^2$ )
Control	$27 \pm 3.23$	$252 \pm 8$	$15.3 \pm 0.5$	$24.4 \pm 0.7$	$4.40 \pm 0.21$
Re 24 h	$13.69 \pm 1.21^*$	$411 \pm 13^*$	$21.6 \pm 1.1^*$	$45.1 \pm 1.9^*$	$14.19 \pm 1.03^*$

Data are expressed as mean $\pm$ SEM. \* $p < 0.05$  vs. the control. Re 24 h, reperfusion for 24 h after OGD.

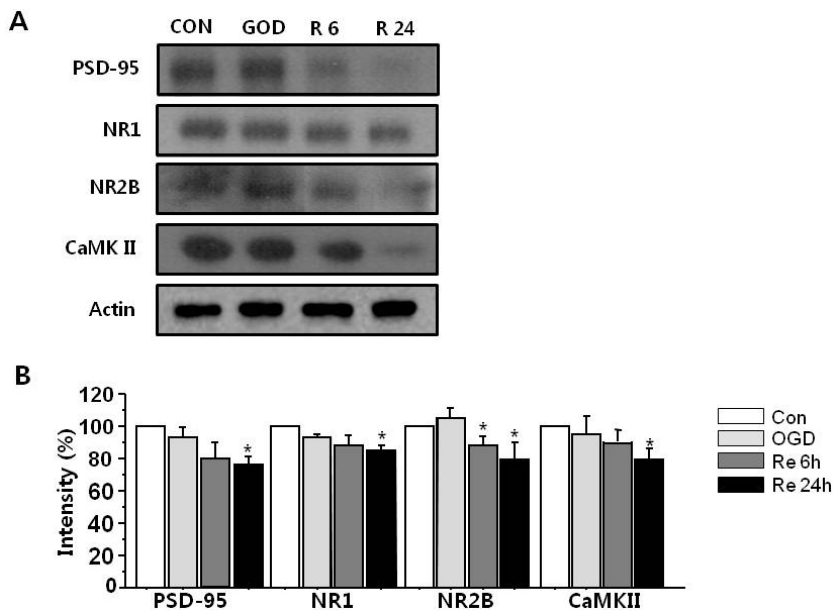


**Fig. 4.** Representative western blots for PSD-95, NR, NR2B, and CaMKII after OGD/reperfusion. (A) At 24 h after OGD, the levels of all the PSD complex proteins were decreased. (B) Data are expressed as mean±SEM. \*p<0.05 vs. the control. n=3.

tochondria, ER, dendrites, and synaptic terminals was observed, and the thickness of PSDs was notably increased. During reperfusion, swelling of cellular organelles and disorganization of the mitochondria was evident. This finding is in agreement with that of other studies, which showed some ultrastructural abnormalities in postischemic neurons, including disaggregation of polyribosomes and deposition of dark substances [44-47].

Changes in synaptic responses after variable periods of hypoxia or ischemia have also been demonstrated frequently both *in vitro* [31,43,48,49] and *in vivo* [50-52]. In this study, OGD/reperfusion induced modifications as shown by EPTA staining for PSD in the CA3 area. At 24 h after OGD, the number of PSDs was significantly decreased, and the remaining PSDs became thicker, longer, and more electron-lucent, reflecting the damage to PSDs. This finding is consistent with that of earlier studies, which demonstrated that dramatic ultrastructural changes to PSDs, along with synaptic deficits occurred following transient ischemia [35,53-55]. Kovalenko et al. [37] reported a rapid increase in the PSD thickness and length, as well as the formation of concave synapses with perforated PSDs in the CA1 stratum radiatum during the first 24 h after an ischemic episode. EPTA primarily stained the synaptic structure and nucleus, but also stained intracellular protein aggregates. After ischemia, EPTA-stained proteins are predominantly accumulated in rat hippocampal CA1 PSDs, a finding which may be attributable to protein unfolding or denaturing exposing their hydrophobic segments during ischemia, and thereby causing interprotein aggregation in the PSDs after ischemia, and resulting in dysfunctional synaptic transmission at the altered synapse. Additionally, unfolding of proteins induced by ischemia may aggregate and change the structure of PSDs, which may lead to loosening of the PSD frame structure, rendering them more diffuse and irregular [56].

In PSDs, the heteromeric combinations of NR1 and NR2A-D interact with PSD-95 and CaMKII [22,57]. Because this complex plays a central role in the regulation of synaptic function [58-60], and is important in linking the syn-

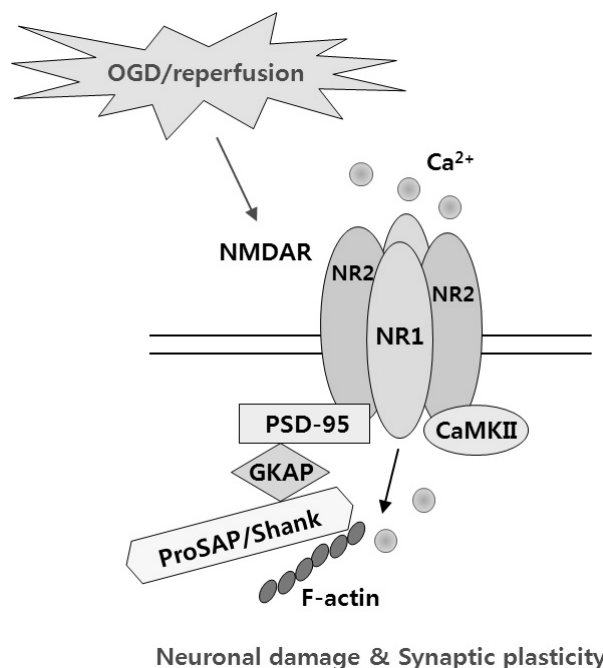


**Fig. 5.** Schematic illustration of the interaction of NMDARs with PSD-95 and CaMKII.

apse to downstream signaling pathways, it could also be involved in the hypoxia/ischemia-induced changes that lead to neuronal damage. Robust morphological alterations to PSD structure after ischemia/reperfusion were accompanied by biochemical changes, such as decreased levels of heat shock cognate protein 70, CaMKII, and protein kinase C in PSDs [55,61]. When western blot analysis for PSD-95, NR1, NR2B, and CaMKII was performed to investigate the relationship between OGD/reperfusion-induced structural modifications of PSDs, and the PSD protein complex, levels



of all the PSD complex proteins were found to be significantly decreased 24 h following OGD (Fig. 5). Previous studies also reported that ischemia/reperfusion [62], or perinatal hypoxia [63] lead to a marked reduction in the mRNA expression of NR1, NR2A, and NR2B, and in the protein expression of PSD-95, total NMDAR levels, and the complexing of PSD-95 with NMDAR subunits within the hippocampal CA1 region, suggesting impaired synaptic performance. Altered PSD-95 expression is centrally involved in the hypoxia-induced changes leading to neuronal injury in the adult brain [55,64].

Taken together, our results show that OGD/reperfusion can induce significant modifications to PSDs in the CA3 area of organotypic hippocampal slice cultures, both morphologically and biochemically. These changes are likely to be part of the process of neuronal cell death and synaptic dysfunction following OGD/reperfusion.

## ACKNOWLEDGEMENTS

We thank Yul A Kim and Jung Mi Han for their excellent technical assistance.

## REFERENCES

1. Arundine M, Chopra GK, Wrong A, Lei S, Aarts MM, MacDonald JF, Tymianski M. Enhanced vulnerability to NMDA toxicity in sublethal traumatic neuronal injury *in vitro*. *J Neurotrauma*. 2003;20:1377-1395.
2. Choi DW. Excitotoxic cell death. *J Neurobiol*. 1992;23:1261-1276.
3. Lipton SA, Rosenberg PA. Excitatory amino acids as a final common pathway for neurologic disorders. *N Engl J Med*. 1994;330:613-622.
4. Lo HM, Hsu KL, Lin FY, Tseng YZ. Implications of prolonged pause in patients with chronic atrial fibrillation with mitral valve disease undergoing atrial compartment operation. *J Formos Med Assoc*. 2003;102:762-767.
5. Jourdain P, Nikonenko I, Alberi S, Muller D. Remodeling of hippocampal synaptic networks by a brief anoxia-hypoglycemia. *J Neurosci*. 2002;22:3108-3116.
6. Nikonenko A, Schmidt S, Skibo G, Brückner G, Schachner M. Tenascin-R-deficient mice show structural alterations of symmetric perisomatic synapses in the CA1 region of the hippocampus. *J Comp Neurol*. 2003;456:338-349.
7. Schmidt-Kastner R, Fliss H, Hakim AM. Subtle neuronal death in striatum after short forebrain ischemia in rats detected by *in situ* end-labeling for DNA damage. *Stroke*. 1997;28:163-169.
8. Cheng D, Hoogenraad CC, Rush J, Ramm E, Schlager MA, Duong DM, Xu P, Wijayawardana SR, Hanfelt J, Nakagawa T, Sheng M, Peng J. Relative and absolute quantification of postsynaptic density proteome isolated from rat forebrain and cerebellum. *Mol Cell Proteomics*. 2006;5:1158-1170.
9. Collins MO, Husi H, Yu L, Brandon JM, Anderson CN, Blackstock WP, Choudhary JS, Grant SG. Molecular characterization and comparison of the components and multiprotein complexes in the postsynaptic proteome. *J Neurochem*. 2006;97 Suppl 1:16-23.
10. Kennedy MB. The postsynaptic density at glutamatergic synapses. *Trends Neurosci*. 1997;20:264-268.
11. Verpelli C, Schmeisser MJ, Sala C, Boeckers TM. Scaffold proteins at the postsynaptic density. *Adv Exp Med Biol*. 2012;970:29-61.
12. Aoki C, Miko I, Oviedo H, Mikeldadze-Dvali T, Alexandre L, Sweeney N, Bredt DS. Electron microscopic immunocytochemical detection of PSD-95, PSD-93, SAP-102, and SAP-97 at postsynaptic, presynaptic, and nonsynaptic sites of adult and neonatal rat visual cortex. *Synapse*. 2001;40:239-257.
13. Friedman HV, Bresler T, Garner CC, Ziv NE. Assembly of new individual excitatory synapses: time course and temporal order of synaptic molecule recruitment. *Neuron*. 2000;27:57-69.
14. Garner CC, Kindler S, Gundelfinger ED. Molecular determinants of presynaptic active zones. *Curr Opin Neurobiol*. 2000;10:321-327.
15. Elias GM, Nicoll RA. Synaptic trafficking of glutamate receptors by MAGUK scaffolding proteins. *Trends Cell Biol*. 2007;17:343-352.
16. Kennedy MB. Signal transduction molecules at the glutamatergic postsynaptic membrane. *Brain Res Brain Res Rev*. 1998;26:243-257.
17. Bredt DS. NO NMDA receptor activity. *Nat Biotechnol*. 1996;14:944.
18. Losi G, Prybylowski K, Fu Z, Luo J, Wenthold RJ, Vicini S. PSD-95 regulates NMDA receptors in developing cerebellar granule neurons of the rat. *J Physiol*. 2003;548:21-29.
19. Roche KW, Standley S, McCallum J, Dune Ly C, Ehlers MD, Wenthold RJ. Molecular determinants of NMDA receptor internalization. *Nat Neurosci*. 2001;4:794-802.
20. Townsend M, Yoshii A, Mishina M, Constantine-Paton M. Developmental loss of miniature N-methyl-D-aspartate receptor currents in NR2A knockout mice. *Proc Natl Acad Sci U S A*. 2003;100:1340-1345.
21. Choi DW. Bench to bedside: the glutamate connection. *Science*. 1992;258:241-243.
22. Kornau HC, Schenker LT, Kennedy MB, Seeburg PH. Domain interaction between NMDA receptor subunits and the postsynaptic density protein PSD-95. *Science*. 1995;269:1737-1740.
23. Niethammer M, Kim E, Sheng M. Interaction between the C terminus of NMDA receptor subunits and multiple members of the PSD-95 family of membrane-associated guanylate kinases. *J Neurosci*. 1996;16:2157-2163.
24. Cull-Candy S, Brickley S, Farrant M. NMDA receptor subunits: diversity, development and disease. *Curr Opin Neurobiol*. 2001;11:327-335.
25. Furukawa H, Singh SK, Mancusso R, Gouaux E. Subunit arrangement and function in NMDA receptors. *Nature*. 2005;438:185-192.
26. Köhr G. NMDA receptor function: subunit composition versus spatial distribution. *Cell Tissue Res*. 2006;326:439-446.
27. Goldenring JR, McGuire JS Jr, DeLorenzo RJ. Identification of the major postsynaptic density protein as homologous with the major calmodulin-binding subunit of a calmodulin-dependent protein kinase. *J Neurochem*. 1984;42:1077-1084.
28. Suzuki T, Okumura-Noji K, Tanaka R, Tada T. Rapid translocation of cytosolic Ca<sup>2+</sup>/calmodulin-dependent protein kinase II into postsynaptic density after decapitation. *J Neurochem*. 1994;63:1529-1537.
29. Malenka RC, Nicoll RA. Long-term potentiation--a decade of progress? *Science*. 1999;285:1870-1874.
30. Okabe S. Molecular anatomy of the postsynaptic density. *Mol Cell Neurosci*. 2007;34:503-518.
31. Jung YJ, Park SJ, Park JS, Lee KE. Glucose/oxygen deprivation induces the alteration of synapsin I and phosphosynapsin. *Brain Res*. 2004;996:47-54.
32. Stoppini L, Buchs PA, Muller D. A simple method for organotypic cultures of nervous tissue. *J Neurosci Methods*. 1991;37:173-182.
33. Ahlgren H, Henjum K, Ottersen OP, Rundén-Pran E. Validation of organotypic hippocampal slice cultures as an *ex vivo* model of brain ischemia: different roles of NMDA receptors in cell death signalling after exposure to NMDA or oxygen and glucose deprivation. *Cell Tissue Res*. 2011;345:329-341.
34. Bloom FE, Aghajanian GK. Fine structural and cytochemical analysis of the staining of synaptic junctions with phosphotungstic acid. *J Ultrastruct Res*. 1968;22:361-375.
35. Hu BR, Janelidze S, Ginsberg MD, Busto R, Perez-Pinzon M, Sick TJ, Siesjö BK, Liu CL. Protein aggregation after focal brain ischemia and reperfusion. *J Cereb Blood Flow Metab*. 2001;21:865-875.

36. Suh EC, Jung YJ, Kim YA, Park EM, Lee KE. A beta 25-35 induces presynaptic changes in organotypic hippocampal slice cultures. *Neurotoxicology*. 2008;29:691-699.
37. Kovalenko T, Osadchenko I, Nikonenko A, Lushnikova I, Voronin K, Nikonenko I, Muller D, Skibo G. Ischemia-induced modifications in hippocampal CA1 stratum radiatum excitatory synapses. *Hippocampus*. 2006;16:814-825.
38. Ruan YW, Han XJ, Shi ZS, Lei ZG, Xu ZC. Remodeling of synapses in the CA1 area of the hippocampus after transient global ischemia. *Neuroscience*. 2012;218:268-277.
39. Mori K, Togashi H, Ueno KI, Matsumoto M, Yoshioka M. Aminoguanidine prevented the impairment of learning behavior and hippocampal long-term potentiation following transient cerebral ischemia. *Behav Brain Res*. 2001;120:159-168.
40. Pulsinelli WA, Brierley JB. A new model of bilateral hemispheric ischemia in the unanesthetized rat. *Stroke*. 1979;10:267-272.
41. Aarts M, Liu Y, Liu L, Besshoh S, Arundine M, Gurd JW, Wang YT, Salter MW, Tymianski M. Treatment of ischemic brain damage by perturbing NMDA receptor- PSD-95 protein interactions. *Science*. 2002;298:846-850.
42. Kirino T, Tsujita Y, Tamura A. Induced tolerance to ischemia in gerbil hippocampal neurons. *J Cereb Blood Flow Metab*. 1991;11:299-307.
43. Park SJ, Jung YJ, Kim YA, Lee-Kang JH, Lee KE. Glucose/oxygen deprivation and reperfusion upregulate SNAREs and complexin in organotypic hippocampal slice cultures. *Neuropathology*. 2008;28:612-620.
44. Kirino T, Robinson HP, Miwa A, Tamura A, Kawai N. Disturbance of membrane function preceding ischemic delayed neuronal death in the gerbil hippocampus. *J Cereb Blood Flow Metab*. 1992;12:408-417.
45. Pulsinelli WA, Levy DE, Duffy TE. Regional cerebral blood flow and glucose metabolism following transient forebrain ischemia. *Ann Neurol*. 1982;11:499-502.
46. Petito CK, Pulsinelli WA. Delayed neuronal recovery and neuronal death in rat hippocampus following severe cerebral ischemia: possible relationship to abnormalities in neuronal processes. *J Cereb Blood Flow Metab*. 1984;4:194-205.
47. Smith ML, Bendek G, Dahlgren N, Rosén I, Wieloch T, Siesjö BK. Models for studying long-term recovery following forebrain ischemia in the rat. 2. A 2-vessel occlusion model. *Acta Neurol Scand*. 1984;69:385-401.
48. Leblond J, Krnjevic K. Hypoxic changes in hippocampal neurons. *J Neurophysiol*. 1989;62:1-14.
49. Lobner D, Lipton P. Intracellular calcium levels and calcium fluxes in the CA1 region of the rat hippocampal slice during in vitro ischemia: relationship to electrophysiological cell damage. *J Neurosci*. 1993;13:4861-4871.
50. Bolay H, Dalkara T. Mechanisms of motor dysfunction after transient MCA occlusion: persistent transmission failure in cortical synapses is a major determinant. *Stroke*. 1998;29:1988-1993.
51. Bolay H, Gürsoy-Ozdemir Y, Sara Y, Onur R, Can A, Dalkara T. Persistent defect in transmitter release and synapsin phosphorylation in cerebral cortex after transient moderate ischemic injury. *Stroke*. 2002;33:1369-1375.
52. Sun FY, Lin X, Mao LZ, Ge WH, Zhang LM, Huang YL, Gu J. Neuroprotection by melatonin against ischemic neuronal injury associated with modulation of DNA damage and repair in the rat following a transient cerebral ischemia. *J Pineal Res*. 2002;33:48-56.
53. Hai J, Yu F, Lin Q, Su SH. The changes of signal transduction pathways in hippocampal regions and postsynaptic densities after chronic cerebral hypoperfusion in rats. *Brain Res*. 2012;1429:9-17.
54. Liu Y, Wong TP, Aarts M, Rooyackers A, Liu L, Lai TW, Wu DC, Lu J, Tymianski M, Craig AM, Wang YT. NMDA receptor subunits have differential roles in mediating excitotoxic neuronal death both in vitro and in vivo. *J Neurosci*. 2007;27:2846-2857.
55. Hu BR, Park M, Martone ME, Fischer WH, Ellisman MH, Zivin JA. Assembly of proteins to postsynaptic densities after transient cerebral ischemia. *J Neurosci*. 1998;18:625-633.
56. Martone ME, Jones YZ, Young SJ, Ellisman MH, Zivin JA, Hu BR. Modification of postsynaptic densities after transient cerebral ischemia: a quantitative and three-dimensional ultrastructural study. *J Neurosci*. 1999;19:1988-1997.
57. Meng FJ, Guo J, Song B, Yan XB, Zhang GY. Competitive binding of postsynaptic density 95 and Ca<sup>2+</sup>-calmodulin dependent protein kinase II to N-methyl-D-aspartate receptor subunit 2B in rat brain. *Acta Pharmacol Sin*. 2004;25:176-180.
58. Yamada M, Saisu H, Ishizuka T, Takahashi H, Abe T. Immunohistochemical distribution of the two isoforms of synaphin/complexin involved in neurotransmitter release: localization at the distinct central nervous system regions and synaptic types. *Neuroscience*. 1999;93:7-18.
59. Yao WD, Gainetdinov RR, Arbuckle MI, Sotnikova TD, Cyr M, Beaulieu JM, Torres GE, Grant SG, Caron MG. Identification of PSD-95 as a regulator of dopamine-mediated synaptic and behavioral plasticity. *Neuron*. 2004;41:625-638.
60. Tsien JZ, Huerta PT, Tonegawa S. The essential role of hippocampal CA1 NMDA receptor-dependent synaptic plasticity in spatial memory. *Cell*. 1996;87:1327-1338.
61. Hu BR, Wieloch T. Persistent translocation of Ca<sup>2+</sup>/calmodulin-dependent protein kinase II to synaptic junctions in the vulnerable hippocampal CA1 region following transient ischemia. *J Neurochem*. 1995;64:277-2784.
62. Liu Z, Zhao W, Xu T, Pei D, Peng Y. Alterations of NMDA receptor subunits NR1, NR2A and NR2B mRNA expression and their relationship to apoptosis following transient forebrain ischemia. *Brain Res*. 2010;1361:133-139.
63. Chen WF, Chang H, Wong CS, Huang LT, Yang CH, Yang SN. Impaired expression of postsynaptic density proteins in the hippocampal CA1 region of rats following perinatal hypoxia. *Exp Neurol*. 2007;204:400-410.
64. Takagi N, Logan R, Teves L, Wallace MC, Gurd JW. Altered interaction between PSD-95 and the NMDA receptor following transient global ischemia. *J Neurochem*. 2000;74:169-178.